

A LENSED ARC IN THE LOW REDSHIFT CLUSTER ABELL 2124<sup>1</sup>

JOHN P. BLAKESLEE AND MARK R. METZGER

Palomar Observatory, California Institute of Technology, Mail Stop 105-24, Pasadena, CA 91125

*To appear in ApJ*

## ABSTRACT

We report the discovery of an arc-like object  $27''$  from the center of the cD galaxy in the redshift  $z = 0.066$  cluster A2124. Observations with the Keck II telescope reveal that the object is a background galaxy at  $z = 0.573$ , apparently lensed into an arc of length  $\sim 8''$  and total R magnitude  $m_R = 20.86 \pm 0.07$ . The width of the arc is resolved; we estimate it to be  $\sim 0''$  after correcting for seeing. A lens model of the A2124 core mass distribution consistent with the cluster galaxy velocity dispersion reproduces the observed arc geometry and indicates a magnification factor  $\gtrsim 9$ . With this magnification, the strength of the [OII]  $\lambda 3727$  line implies a star-formation rate of  $\text{SFR} \sim 0.4 h^{-2} M_\odot \text{ yr}^{-1}$ . A2124 thus appears to be the lowest redshift cluster known to exhibit strong lensing of a distant background galaxy.

*Subject headings:* galaxies: clusters: individual (Abell 2124) — galaxies: elliptical and lenticular, cD — gravitational lensing

## 1. INTRODUCTION

The vast majority of known gravitational arcs have been identified in galaxy clusters at redshifts  $z > 0.2$  (see for instance the tabulations by LeFèvre *et al.* 1994 and Kneib & Soucail 1996). They have been used to place constraints on the mass distributions within these clusters free from any assumptions regarding hydrostatic or dynamical equilibrium (Narayan & Bartelmann 1998 give a recent review). Such instances of strong lensing also provide the opportunity to study the properties of the distant background galaxies that are magnified by the foreground cluster lenses.

One cluster with  $z < 0.1$  proposed to exhibit a gravitational arc is A3408 at  $z = 0.042$  (Campusano & Hardy 1996). Campusano, Kneib, & Hardy (1998) further investigated the possibility that the spiral galaxy at  $z = 0.073$  located  $50''$  from the central elliptical in A3408 is being lensed. They found that the lensing must be fairly weak, with a magnification factor  $\lesssim 1.7$ . Even so, lensing in low-redshift clusters in general provides the opportunity to study core mass distributions at higher spatial resolutions than that afforded by the moderate to high-redshift clusters that have been the focus of most lensing studies so far.

Abell 2124 is a richness class 1 cluster at a redshift  $z = 0.066$ . Hill & Oegerle (1993) measured velocities for 66 galaxies with  $17,800 < cz < 23,700 \text{ km s}^{-1}$  in the field of A2124 and reported a cluster dispersion of  $\sigma_{cl} = 1180 \text{ km s}^{-1}$ ; they noted that the high dispersion was primarily due to four galaxies with  $cz \sim 23,500 \text{ km s}^{-1}$ . Fadda *et al.* (1996) reanalyzed the velocity data and concluded  $\sigma_{cl} = 878_{-72}^{+90} \text{ km s}^{-1}$  from 61 cluster members. This latter value is more appropriate to A2124's fairly modest X-ray luminosity  $L_X = 1.4 \times 10^{44} \text{ ergs s}^{-1}$  in the 0.1–2.4 keV band (Ebeling *et al.* 1996). However, the cluster velocity dispersion profile shown by Fadda *et al.* appears to rise to  $\sigma_{cl} \gtrsim 1100 \text{ km s}^{-1}$  within

$r \lesssim 100 h^{-1} \text{ kpc}$  (where  $h$  is the Hubble constant in units of  $100 \text{ km s}^{-1} \text{ Mpc}^{-1}$ ).

As a Bautz-Morgan type I, Rood-Sastry class cD cluster (Abell *et al.* 1989; Struble & Rood 1987), A2124 is dominated by a single giant cD galaxy, UGC 10012. The cD has a central stellar velocity dispersion of  $305 \pm 15 \text{ km s}^{-1}$  and a “secondary nucleus” at a projected separation of  $11.2 h^{-1} \text{ kpc}$  with a relative velocity of  $949 \pm 14 \text{ km s}^{-1}$  (Blakeslee & Tonry 1992). The cD itself has no significant peculiar velocity with respect to the cluster mean (Oegerle & Hill 1994).

## 2. OBSERVATIONS

We observed the A2124 cD as part of a project to extend to larger distances and denser environments a previous survey of the globular cluster populations of brightest cluster galaxies (Blakeslee, Tonry, & Metzger 1997). In the course of inspecting the final image, we noticed a narrow arc-like object  $27''$  along the major axis from the cD center. The orientation of the arc suggested that it might be lensed, so we carried out further observations to test this hypothesis.

## 2.1. Imaging Data

The cD galaxy in A2124 was imaged in the *R* band on the night of 28 April 1997 with the Low Resolution Imaging Spectrograph (LRIS, Oke *et al.* 1995) on the Keck II telescope under photometric conditions. The image scale was  $0''.211 \text{ pix}^{-1}$ . As the goal was to detect faint globular clusters in the cD halo, the total integration time was 8400 s; the seeing in the final stacked image was  $0''.57$ . The data were reduced as detailed by Blakeslee *et al.* (1997). The photometric calibration of the image, determined from Landolt (1992) standard stars observed the same night, agreed to within 0.01 mag with that of a short *R*-band photometric exposure taken with COSMIC (Dressler 1993) on the Palomar 5 m telescope.

Figure 1 shows the central  $3'$  of the deep 8400 s *R*-band Keck image. The arc is located  $26''.9 \pm 0''.2$  from the cen-

<sup>1</sup>Based on observations obtained at the W.M. Keck Observatory, operated as a scientific partnership by the California Institute of Technology, the University of California, and the National Aeronautics and Space Administration.

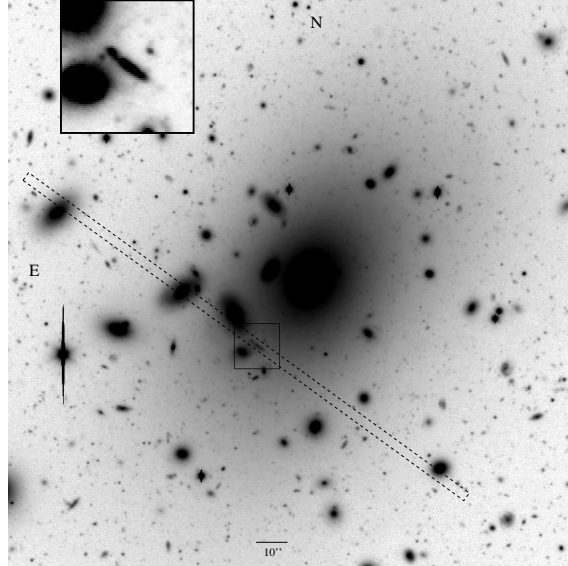


FIG. 1.— The central  $3 \times 3$  arcminutes of the 8400 s LRIS  $R$ -band image centered near the A2124 cD is displayed with a logarithmic stretch. The dotted line shows schematically the placement of the LRIS slit for the spectroscopic observations presented here. A  $14'' \times 14''$  box drawn around the arc is enlarged by a factor of three in the inset. The inset uses a linear stretch and has had a smooth background fit to the cD halo subtracted.

ter of the cD at a position angle  $PA = 141^\circ$ , very close to the major axis of the cD. The elliptical cD isophotes at radii  $r_{\text{maj}} \geq 19''$  along the major axis are oriented at  $PA = 144^\circ \pm 1^\circ$ . (At  $r_{\text{maj}} < 10''$ , the cD isophotes are at  $PA \approx 157^\circ$  and are less elliptical.) The cD halo has a surface brightness  $\mu_R = 22.9 \text{ mag arcsec}^{-2}$  at the position of the arc.

The isophotal contour map plotted in Figure 2 reveals substructure in the A2124 arc. The brightest intensity peak is located near the arc center, with two fainter peaks near either end of the main part of the arc. A faint tail extends  $\sim 1''.5$  further to the southwest along the same line as the main part of the arc. There is a stellar object located  $1''.2$  to the southeast of the intensity peak at the northeast end of the arc; because it does not follow the same locus, we believe this object is unassociated with the arc (compare the inset in Figure 1). Its magnitude  $m_R \sim 24.5$  corresponds to the brightest globular clusters in the cD. After all sources of contamination are accounted for, and corrected for 0.07 mag of Galactic extinction (Schlegel, Finkbeiner, & Davis 1998), the total  $R$  magnitude of the arc is  $m_R(\text{arc}) = 20.86 \pm 0.07$ .

The axis ratio of the arc is poorly defined because of the substructure. The axis ratio of the 23.4 mag  $\text{arcsec}^{-2}$  isophote (about half the intensity of the brightest isophote plotted) is 4.8, and would be  $\sim 5.7$  in the absence of seeing. However, the total length of the arc including the faint tail to the southwest is at least  $8''.5$ , and the full width at half maximum normal to the arc at the central or northeast intensity peaks is  $\text{FWHM} = 0''.83 \pm 0''.04$ , which would be  $\text{FWHM} \sim 0''.6$  in the absence of seeing. Using these measures, the axis ratio is then  $l/w \sim 14$ . By measuring the deviation from lines drawn from one end of the arc to the other, we estimate the radius of curvature to be  $100'' \pm 20''$ .

We also obtained  $4 \times 400$  s of  $B$ -band integration with COSMIC on the Palomar 5 m. The seeing in the stacked  $B$  image was  $1''.7$ , making it difficult to measure an ac-

curate color. For the brightest  $7''$  of the arc, we find  $(B-R)_0 = 1.85 \pm 0.25$ .

## 2.2. Spectroscopic Data

We obtained two 900 s spectra of the arc with LRIS on the night of 18 June 1998. A 300 line grating blazed at 5000 Å gave a dispersion of  $2.44 \text{ \AA pix}^{-1}$  and wavelength coverage of 4000–9000 Å. The slit was  $1''$  wide, yielding a resolution of  $\sim 10 \text{ \AA}$ . The slit was oriented at a PA of  $54^\circ 1'$ , aligned with the bright nucleus of the S0 galaxy  $30''$  northeast of the arc, as shown in Figure 1. The alignment galaxy has an absorption spectrum that indicates it is an A2124 member at  $z = 0.0652$ . Halogen flats and arc-lamp exposures were taken after each spectrum, and standard IRAF routines were used for extraction and wavelength calibration. The spectra were flux calibrated using a spectrum of Feige 110 taken at the end of the night. Variable seeing and the presence of thin, patchy cirrus makes the absolute calibration uncertain.

The raw two-dimensional spectra show one bright emission line at the spatial position of the arc, tilted obliquely with respect to the night sky lines. The tilt is at least partly the result of the misalignment of the arc and the slit. On close inspection of the sky-subtracted 2-d spectra, two other much weaker emission lines are visible at longer wavelengths with the same tilt as the brighter line. The total tilt is consistent with the width of the slit, and the length of the emission in the spatial direction is consistent with the length of the main part of the arc in the  $R$ -band image. This indicates that the arc was well-centered within the slit and that the seeing was somewhat better than  $1''$ .

Figure 3 shows the final calibrated 1-d spectrum of the arc. Identifying the strong emission line at 5863.5 Å with [OII]  $\lambda 3727.5 \text{ \AA}$  gives a redshift  $z = 0.5730 \pm 0.0002$ . Identifying the line observed at  $7798.2 \text{ \AA}$  as [OII]  $\lambda 5006.9$  gives  $z = 0.5723 \pm 0.0005$ . Unfortunately,  $H\beta$  lands in the midst of the atmospheric absorption of the Fraunhofer  $A$  band.

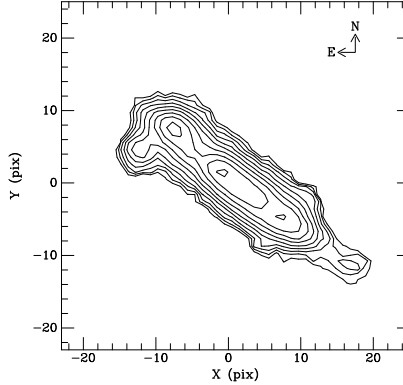


FIG. 2.— The isophotal contour map of the A2124 arc. Contours are drawn in 0.4 mag increments with the brightest at  $\mu_R = 22.5$  mag arcsec $^{-2}$  and the faintest at  $\mu_R = 26.1$  mag arcsec $^{-2}$ . A sky background of 20.69 mag arcsec $^{-2}$  has been subtracted, and contributions from all other sources of light have been removed by masking out the arc and interpolating across it. Because of the bright background, the precise values of the faintest isophotes plotted are fairly uncertain. The size of the map is 10''  $\times$  10''.

There does appear to be real emission (as evidenced by the 2-d spectrum) corresponding to H $\beta$  at  $z = 0.5729$ , but the irregular profile of the  $A$  band makes the precise position unreliable. The other Balmer features identified in the figure give an average  $z \sim 0.5726$ . Relying mainly on the [OII] line and including calibration uncertainty, we adopt a redshift  $z_{\text{arc}} = 0.5728 \pm 0.0003$ .

We can identify some other absorption features in the arc spectrum. Mg  $b$  absorption is visible around  $\sim 8135$  Å, in a gap between night sky emission lines. The Ca  $K$  absorption line appears weaker than the Ca  $H$  line because the latter is blended with He. Similarly, there is not a strong 4000 Å break, but there is a change in spectral slope corresponding to the Balmer limit near 5735 Å.

In comparison to the galaxy spectra in the atlases of Kennicutt (1992a) and Liu & Kennicutt (1995), the A2124 arc spectrum most resembles those of the “post-starburst” galaxies suggested to be the local analogs of distant E+A galaxies. These are low ionization systems that may have strong [OII] and H $\alpha$  (off the end of our spectrum) emission from ongoing star formation, sometimes show weak emission at H $\beta$  and H $\gamma$ , but have the rest of the Balmer series appearing strongly in absorption; they are thought to be evolved merger events. This is what we see, although the [OII] equivalent width measured for the arc  $\text{EW}_{\text{[OII]}} = 30.1 \pm 1.6$  Å would place it among the youngest of these “post-starburst” galaxies.

### 3. LENS MODELS

To model the cluster as a lens, we use an elliptical potential of the form (Blandford & Kochanek 1987)

$$\psi(r') = 4\pi \left(\frac{\sigma_{1D}}{c}\right)^2 \frac{D_{LS}}{D_S} \left[ \left(1 + \frac{r'^2}{r_c^2}\right)^{\frac{1}{2}} - 1 \right],$$

where  $\sigma_{1D}$  is the line-of-sight velocity dispersion in the limit  $r' \gg r_c$  for the spherical case,  $D_S$  and  $D_{LS}$  are angular size distances to the source and from the lens to the source, respectively, and  $r_c$  defines a softening radius. The ellipticity enters in the definition of  $r'$ ,

$$r'^2 = (1 - \epsilon_p)x^2 + (1 + \epsilon_p)y^2,$$

where the coordinates  $x, y$  are aligned along the major and minor axes of the potential. This represents a softened isothermal sphere for  $\epsilon_p = 0$ , and tends to represent the shape of dark halo potentials fairly well near the cores of clusters (e.g., Tyson *et al.* 1998). We chose the more limited relation with a fixed power law, as there are few lensing constraints in this system to differentiate various potential profiles.

We also chose to fix many of the model parameters using observational constraints where available. The orientation and ellipticity of the cluster potential were set based on the measured  $\theta_l, \epsilon_l$  of cD halo light profile, using the approximation  $\epsilon_p = \epsilon_l/3$ , following Mellier *et al.* (1993). The center of the cluster potential was fixed at the cD center. Two additional spherical terms with  $r_c = 0''.2$  were added to represent the central cusp of the cD itself and the halo of the bright galaxy 12'' northeast of the arc. The cD potential was normalized by setting the asymptotic dispersion  $\sigma_{1D} = 305$  km s $^{-1}$  from the measured central dispersion (Blakeslee & Tonry 1992), and  $\sigma_{1D} = 180$  km s $^{-1}$  was assumed for the bright galaxy.

Our primary constraints for the lens model are the arc radius, size, and orientation. The lack of a counterarc suggests a source position that lies outside the tangential and radial caustics (e.g., Grossman & Narayan 1988). However, the length of the arc could imply either a much longer arc opposite that is not observed, or a shorter de-magnified arc that would be ambiguous without redshift information.

A family of models with a range of core radii and asymptotic dispersions for the primary lens (cluster dark matter) were found that reproduce the characteristics of the arc. These models are degenerate in  $\sigma_{1D}$  and  $r_c$  for determining the mass enclosed within the arc radius. Models with large core radii tend to produce larger radial magnifications, leading to smaller intrinsic source sizes and larger total magnifications. Fixing the velocity dispersion to the Fadda *et al.* (1996) value of 878 km s $^{-1}$ , we find a best-fit model having  $r_c = 10''$  (9  $h^{-1}$  kpc) and a roughly round source 0''.4 in extent with an unlensed position 6''.1 east and 6''.8 south of the cD center. Figure 4 shows the source and image planes for this model, along with the caustic and critical curve structure. The magnification of the source ranges between 9 and 13 for the family of best-fit models.

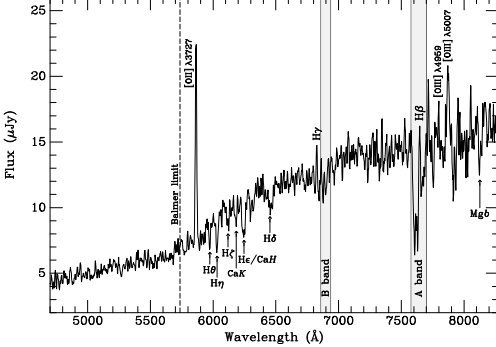


FIG. 3.— The sky-subtracted, calibrated 1-d spectrum of the arc, smoothed with a 7.5 Å wide boxcar filter. The shaded regions enclose the atmospheric *A* and *B* absorption bands. The strong [OII]  $\lambda 3727$  line observed at 5863 Å yields a redshift  $z_{\text{arc}} = 0.573$ . The [OIII]  $\lambda 5007$  line is clearly detected, but is much weaker than  $\lambda 3727$  and somewhat obscured by residuals from the numerous OH sky lines; [OIII]  $\lambda 4959$  may also be present at a low level. H $\beta$  is redshifted into the *A* band, but the putative emission has the same spatial signature as do the  $\lambda 3727$  and  $\lambda 5007$  lines, and thus is apparently real. A spike is visible at the redshifted position of H $\gamma$ , but the higher order Balmer lines appear in absorption. Mg $\delta$  absorption, indicating an older stellar component, lands in a gap between sky emission lines and is visible. The positions of the Ca I *H* & *K* lines and the Balmer limit are also shown.

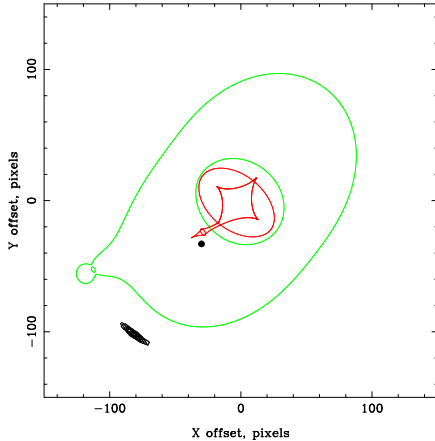


FIG. 4.— One of the best-fitting models of the Abell 2124 arc. The cD lies at (0,0), and the coordinates are in units of LRIS pixels ( $0''.211 \text{ pix}^{-1}$ ) with north up and east to the left. The black contours indicate surface brightness of the source and image; the caustics (critical surfaces in the source plane) are shown in red, and the critical curves are shown in green.

#### 4. DISCUSSION

We find that quite reasonable values of the physical parameters of the cluster and source can naturally produce a lensed arc at the observed radius. Though our best-fit core radius for the cluster may seem small, it has been shown that cluster potentials as measured by lensing in higher redshift clusters tend to be steeper near the center than implied by models of the X-ray emission (LeFèvre *et al.* 1994; Waxman & Miralda-Escude 1995). The intrinsic dispersion of this cluster is also somewhat ambiguous, and adopting dispersions nearer the larger estimate (§1) implies larger core radii. The core radius is not strongly affected by changing the model of the cD potential, which is a relatively small perturbation on the cluster potential. There are several faint sources in the field that appear arc-like and may be strongly lensed; having arcs at different radii would allow better constraints on the slope of the potential near the core.

At  $z=0.573$  and in the absence of lensing,  $1''$  corresponds to  $4.3\text{--}3.7 h^{-1} \text{ kpc}$  ( $q_0=0\text{--}0.5$ ). The observed  $8''.5$

arc length would then imply a physical length of 53 kpc (for  $q_0=0$ ,  $h=0.7$ ), or 64 kpc ( $q_0=h=0.5$ ). With a *k*-correction of  $-0.4$  mag, the observed magnitude  $m_R = 20.86$  would correspond to  $M_R \approx -21.3 + 5 \log(h)$ , nearly  $2L^*$  (Lin *et al.* 1996, with  $R-r = -0.3$ ). The observed ( $B-R$ ) color is that of an “E+A” galaxy in which the merger/starburst occurred  $\lesssim 0.5$  Gyr ago (Belloni *et al.* 1995; Belloni & Röser 1996).

We noted that the arc’s spectrum resembles that of some “post-starburst” galaxies. From the observed [OII] emission, we can infer the ongoing star-formation rate (SFR). The total [OII]  $\lambda 3727$  line flux in the spectrum shown in Figure 3 is  $(1.89 \pm 0.05) \times 10^{-16} \text{ ergs s}^{-1} \text{ cm}^{-2}$ . We estimate the total flux to be larger by 15–20% due to the placement of the arc in the slit and the better seeing for the flux standard spectrum. However, the presence of thin cirrus makes the absolute flux uncertain by at least another 10%. We therefore conservatively adopt  $f_{[\text{OII}]} = (2.1 \pm 0.3) \times 10^{-16} \text{ ergs s}^{-1} \text{ cm}^{-2}$ . This translates to a luminosity  $L_{[\text{OII}]} = (1.2 \pm 0.2) \times 10^{41} h^{-2} \text{ ergs s}^{-1}$ . Adopting the mean relation from Kennicutt (1998) and

setting  $h = 0.7$  yields  $\text{SFR} = 8.5 \pm 3.3 \text{ M}_\odot \text{ yr}^{-1}$ . The SFR calibration based on [OII] equivalent width and observed  $B$  luminosity (Kennicutt 1992b, modified as in Kennicutt 1998) is intrinsically much less certain but gives a similar result.

The  $z = 0.573$  galaxy would thus be an extremely large and luminous, linear or flattened galaxy with a lumpy morphology and a substantial amount of ongoing star formation. These points would be indicative of a large merger event, except for the narrow, slightly curved shape. The extreme length if unlensed (50–65 kpc) by itself suggests that the arc is a gravitationally magnified image of a smaller object with a more modest SFR.

Further observations might help to confirm the lens model and constrain the cluster mass profile at small physical radii. A weak lensing analysis would help to determine the radial mass profile; such an analysis is in progress but complicated by the extensive globular cluster population. A2124 would be an ideal target for a wide-field imager on a 4m class telescope (e.g., Boroson *et al.* 1994; Metzger, Luppino, & Miyazaki 1995). A search for a counterarc via longslit spectroscopy might prove fruitful, since the acceptable image positions would lie roughly along a line. The demagnification in models with additional images yields sources not much fainter than  $R = 24$ , and given the strong emission line in the lensed galaxy, this could be detected with Keck spectroscopy. In addition, HST observations of the arc and possible additional arcs might show substructure that would provide further lens mapping constraints.

## 5. SUMMARY AND CONCLUSIONS

We have identified an arc-like object at  $z = 0.573$  located  $27''$  along the major axis from the center of the cD

galaxy in A2124 ( $z = 0.066$ ). The total magnitude of the arc is  $m_R = 20.86 \pm 0.07$ , corrected for Galactic extinction, and the color is  $(B-R)_0 = 1.85 \pm 0.25$ . There are three intensity peaks along its length and a faint extension  $\sim 1''.5$  to the southwest that makes the total length  $8''.5$ , and the axis ratio  $\sim 14$ . The spectrum shows strong [OII] emission with  $\text{EW}_{\text{[OII]}} = 30.1 \pm 1.6 \text{ \AA}$  and strong higher-order Balmer absorption; it thus resembles the spectra of some “post-starburst” galaxies. If the object were unlensed, the observed length would correspond to a physical size of  $\sim 50$ –65 kpc, and the observed [OII] emission would imply  $\text{SFR} = 8.5 \pm 3.3 \text{ M}_\odot \text{ yr}^{-1}$  ( $h = 0.7$ ). We believe it is more likely that the arc is the magnified image of a smaller background object, and the true SFR is less than a tenth of this. A simple lens model, appropriate to the core of A2124, produces an arc radius equal to that observed. This model and the observed geometry strongly support the lensing hypothesis for the A2124 arc; further observations may yield additional constraints that could confirm or reject this hypothesis. Finally, as the probability of such distant galaxies being lensed by nearby clusters depends on the poorly-known shape of the inner cluster potential, it would be worthwhile to try to find these lenses in a systematic, rather than serendipitous, manner.

We thank Terry Stickel and Teresa Chelminiak for assistance at the telescope and Judy Cohen, Bev Oke, and the rest of the team responsible for the Low Resolution Imaging Spectrograph. We also thank C.-P. Ma for valuable discussions. Keck Observatory was made possible by the generous financial support of the W.M. Keck Foundation. J.P.B. is grateful to the Sherman Fairchild Foundation for support. M.R.M’s research was supported by Caltech.

## REFERENCES

Abell, G. O., Corwin H. G. Jr. & Olowin, R. P. 1989, *ApJS*, 70, 1  
 Belloni, P., Bruzual, A. G., Thimm, G. J., & Röser, H.-J. 1995, *A&A*, 297, 61  
 Belloni, P. & Röser, H.-J. 1996, *A&A*, 118, 65  
 Blakeslee, J. P. & Tonry, J. L. 1992, *AJ*, 103, 1457  
 Blakeslee, J. P., Tonry, J. L., & Metzger, M. R. 1997, *AJ*, 114, 482  
 Blandford, R. D. & Kochanek, C. S. 1987, *ApJ*, 321, 658  
 Boroson, T., Reed, R., Wong, W.-Y., & Lesser, M. 1994, *Proc. SPIE*, 2198, 877  
 Campusano, L. D. & Hardy, E. 1996, in *Astrophysical Applications of Gravitational Lensing*, ed. C. S. Kochanek & J. N. Hewitt (Dordrecht: Kluwer), 125  
 Campusano, L. D., Kneib, J.-P., & Hardy, E. 1998, *ApJ*, 496, L79  
 Dressler, A. 1993, in *Palomar Obs. Ann. Rep.* 1993, 2  
 Ebeling, H., Voges, W., Bohringer, H., Edge, A. C., Huchra, J. P., Briel, U. G. 1996, *MNRAS*, 281, 799  
 Fadda, D., Girardi, M., Giuricin, G., Mardirossian, F., Mezzetti, M. & Biviano, A. 1996, *ApJ*, 473, 670  
 Grossman, S. A. & Narayan R. 1988, *ApJ*, 324, L37  
 Hill, J. M. & Oegerle, W. R. 1993, *AJ*, 106, 831  
 Kennicutt, R. C. 1992a, *ApJS*, 79, 255  
 Kennicutt, R. C. 1992b, *ApJ*, 388, 310  
 Kennicutt, R. C. 1998, *ARA&A*, 36, in press  
 Kneib, J.-P. & Soucail, G. 1996, in *Astrophysical Applications of Gravitational Lensing*, ed. C. S. Kochanek & J. N. Hewitt (Dordrecht: Kluwer), 113  
 Landolt, A. U. 1992, *AJ*, 104, 340  
 LeFèvre, O., Hammer, F., Angonin, M. C., Gioia, I. M., & Luppino, G. A. 1994, *ApJ*, 422, L5  
 Lin, H., Kirshner, R. P., Shectman, S. A., Landy, S. D., Oemler, A., Tucker, D. L., & Schechter, P. L. 1996, *ApJ*, 464, 60  
 Liu, C. T. & Kennicutt, R. C. 1995, *ApJS*, 100, 325  
 Mellier, Y., Fort, B., & Kneib, J.-P. 1993, *ApJ*, 407, 33  
 Metzger, M. R., Luppino, G. A., & Miyazaki, S. 1995, *BAAS*, 187, 7305  
 Narayan, R. & Bartelmann, M. 1998, in *Proc. 1995 Jerusalem Winter School, Formation of Structure in the Universe*, ed. A. Dekel & J. P. Ostriker (Cambridge: Cambridge Univ. Press)  
 Oegerle, W. R. & Hill, J. M. 1994, *AJ*, 107, 857  
 Oke, J. B., Cohen, J. G., Carr, M., Cromer, J., Dingizian, A., Harris, F. H., Labrecque, S., Lucinio, R., Schaaf, W., Epps, H., & Miller, J. 1995, *PASP*, 107, 307  
 Schlegel, D., Finkbeiner, D., & Davis, M. 1998, *ApJ*, 500, 525  
 Struble, M. F. & Rood, H. J. 1987, *ApJS*, 63, 555  
 Tyson, J. A., Kochanski, G. P., & Dell’Antonio, I. P. 1998 *ApJ*, 498 L107  
 Waxman, E. & Miralda-Escude, J. 1995, *ApJ*, 451, 451